Strength tests of glulam beams with quadratic holes - Test report

Danielsson, Henrik

2008

LUND UNIVERSITY

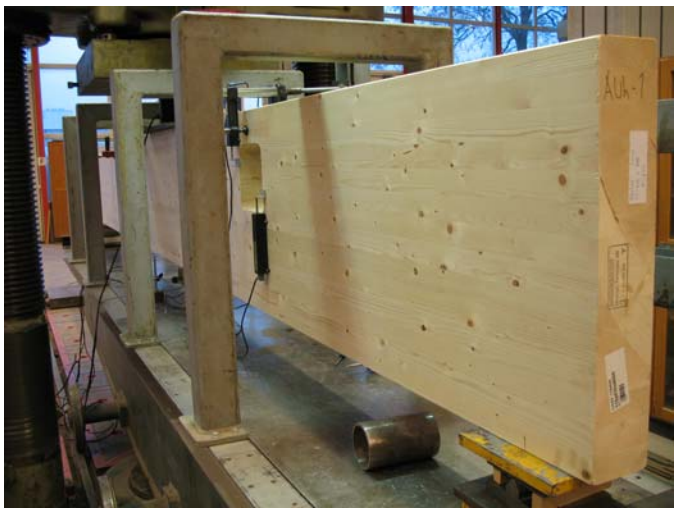

STRENGTH TESTS OF GLULAM BEAMS WITH QUADRATIC HOLES - TEST REPORT

HENRIK DANIELSSON

Structural Mechanics

Department of Construction Sciences
Structural Mechanics

ISRN LUTVDG/TVSM--08/7153--SE (1-29)
ISSN 0281-6679

STRENGTH TESTS OF GLULAM BEAMS WITH QUADRATIC HOLES - TEST REPORT

HENRIK DANIELSSON

Printed by KFS i Lund AB, Lund, Sweden, March 2008.

For information, address:
Division of Structural Mechanics, LTH, Lund University, Box 118, SE-221 00 Lund, Sweden.
Homepage: http://www.byggmek.lth.se

Abstract

This report deals with strength tests of glulam beams with quadratic holes with rounded corners. A total of 36 individual tests were carried out, divided into nine test series with four nominally equal tests in each test series. There were four parameters varied within these test series: beam size, bending moment to shear force ratio, material strength class and also hole placement with respect to the height of the beam. The latter parameter seems to never have been investigated before since all previously performed tests found in the literature have been carried out on beams with holes placed centrically in the beam height direction. The test results indicate a strong size effect. The influence of eccentric placement of the hole on the crack load was found to be small.

Keywords: glulam, hole, strength, test, size effect, eccentric hole.

Acknowledgements

The work presented in this report was carried out at the Division of Structural Mechanics at Lund University during the winter of 2007/2008. The financial support through collaboration with Ulf Arne Girhammar at Umeå University within the project *Multi-story timber frame buildings* (The European Union's Structural Funds – Regional Fund: Goal 1) and from *Formas* through grant 24.3/2003-0711 is greatly appreciated. I would also like to acknowledge *Svenskt Limträ AB* for assisting the project by supplying all glulam beams. I would furthermore like to give special thanks to my supervisor Per Johan Gustafsson, Roberto Crocetti at Moelven Töreboda AB and research engineers Per-Olof Rosenkvist and Thord Lundgren for valuable contributions during the work with this project.

Lund, February 2008

Henrik Danielsson

Contents

1 Introduction

The tests presented in this report deals with the strength of glulam beams with holes. A total of 36 individual tests were carried out, divided into nine test series with four nominally equal tests in each test series. All holes were quadratic with rounded corners and with a side length equal to one third of the beam height. The study comprises investigations of primarily two interesting and potentially important design variables: *beam size effect* and *hole placement with respect to beam height*. Two other design parameters are also studied to some extent: *material strength class* and *bending moment to shear force ratio* at hole center.

Beam size
: Two different beam cross section sizes were used within the test series, 115×180 mm^2 and 115×630 mm^2, in order to investigate the size dependence of the strength.

Hole placement with respect to beam height
: Three different hole placements with respect to the height of the beam were tested, centrically placed holes and holes placed with its center in the upper or lower part of the beam respectively.

Material Strength Class
: Two different material strength classes were used, homogeneous glulam of lamination strength class LS22 and combined glulam of lamination strength classes LS22 and LS15.

Bending moment to shear force ratio
: Two different test setups were used concerning the bending moment to shear force ratio, one with the hole center placed in a position (in the length direction of the beam) with a combined state of shear force and bending moment and another setup where the hole is placed with its center at a point of zero bending moment.

Different hole placements with respect to the beam height seems to never have been investigated before since all previously performed tests found in the literature have been carried out on beams with holes placed centrically with respect to the beam height [1].

The report is organized in the following way. The nine test series and the different test setups, test procedures, recorded measures and other characteristics of the tests are presented in Section 2. The glulam beams are described concerning material strength class, lamellae size, density, moisture content and other material properties in Section 3. The results of the strength tests are presented in Section 4 and some concluding remarks on the results are given in Section 5.

2 Test series

The test series are in Table 1 described concerning name, number of tests, test setup, hole placement, strength class type, beam size and hole size. The geometric properties and the bending moment to shear force ratios at hole center for Test Setup 1 and Test Setup 2 are illustrated in Figure 1. The names of the test series consist of a three letter combination. All tests with the same first letter (A, B, C, D) have the same test setup and geometry with the exception of the hole placement which is described by the second letter (M=Middle, U=Upper, L=Lower) according to Figure 1. The last letter of the combination tells whether the beams are strength class homogeneous (h) or strength class combined (c).

Table 1: *Test series.*

Test series	Number of tests	Test setup	Hole placement	Strength class type	Beam size $T \times H$ [mm^2]	Hole size $a \times b$ [mm^2]	r [mm]
AMh	4	1	Middle	homogeneous	115×630	210×210	25
AMc	4	1	Middle	combined	115×630	210×210	25
AUh	4	1	Upper	homogeneous	115×630	210×210	25
ALh	4	1	Lower	homogeneous	115×630	210×210	25
BMh	4	2	Middle	homogeneous	115×630	210×210	25
CMh	4	1	Middle	homogeneous	115×180	60×60	7
CUh	4	1	Upper	homogeneous	115×180	60×60	7
CLh	4	1	Lower	homogeneous	115×180	60×60	7
DMh	4	2	Middle	homogeneous	115×180	60×60	7

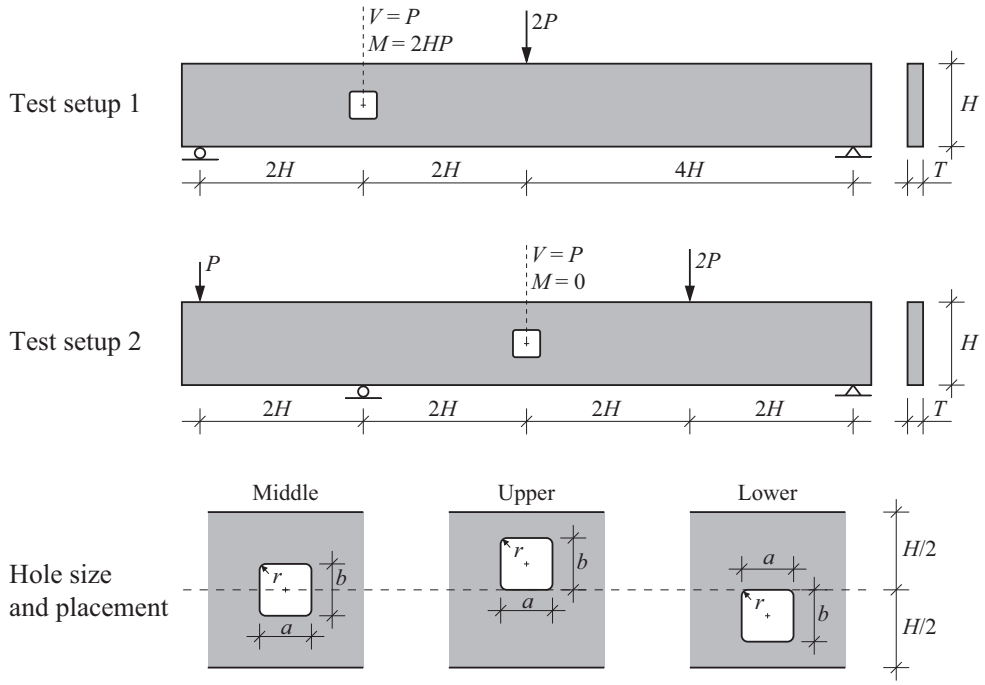

Figure 1: *Test setups and hole placements.*

All tests were run in deformation control. The rate of total deformation was 0.02 mm/s for test series AMh (except AMh-1 were the rate was 0.05 mm/s), AMc, AUh, ALh and BMh while the rate of total deformation was 0.007 mm/s for test series CMh, CUh, CLh and DMh. These rates resulted in a test duration of approximately 20-30 minutes. The rate of total deformation referred to is the rate of the actuator in the testing machine. These rates of total deformations allowed careful observations of the two corners of the holes where cracks were expected during the loading procedure which enabled a careful investigation of the initiation and propagation of the cracks.

The following variables were recorded for all tests: the total deformation, applied load P, beam deflection δ and also vertical deformations d in the beam at the two failing corners of the hole. Four LVDT sensors were used to measure these deformations, one on each side of the beam at the two failing corners of the hole. A fifth LVDT sensor was used to measure the beam deflection δ. The placement of these sensors, glulam beam sizes and sizes of steel beams and support plates are shown in Figures 2 and 3.

For test series AMh, AMc, AUh, ALh, CMh, CUh and CLh the glulam beams were delivered with a total length which was longer than the span length of the test setup and there where two holes in each beam as shown in Figure 3. Hence, two test were performed on the same beam. For these test series, tests 1 and 2 and tests 3 and 4 were performed on the same beam. The larger beams ($H = 630$ mm) were by means of a roller type of support stabilized in the weak direction at three points along the beam length. Photos of the hole and the LVDT sensors are for some tests shown in Figure 4. Photos of the test setups used for the nine different test series are shown in Figure 5.

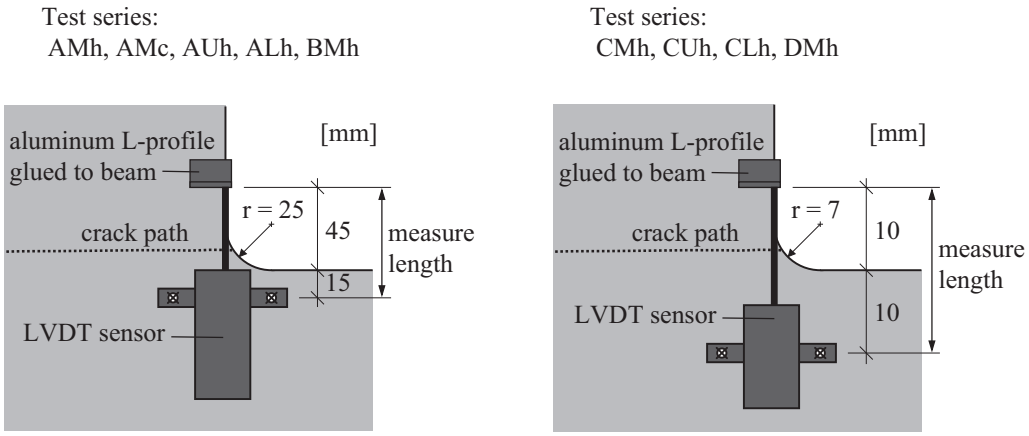

Figure 2: *Placement of LVDT sensors for measurement of deformation d.*

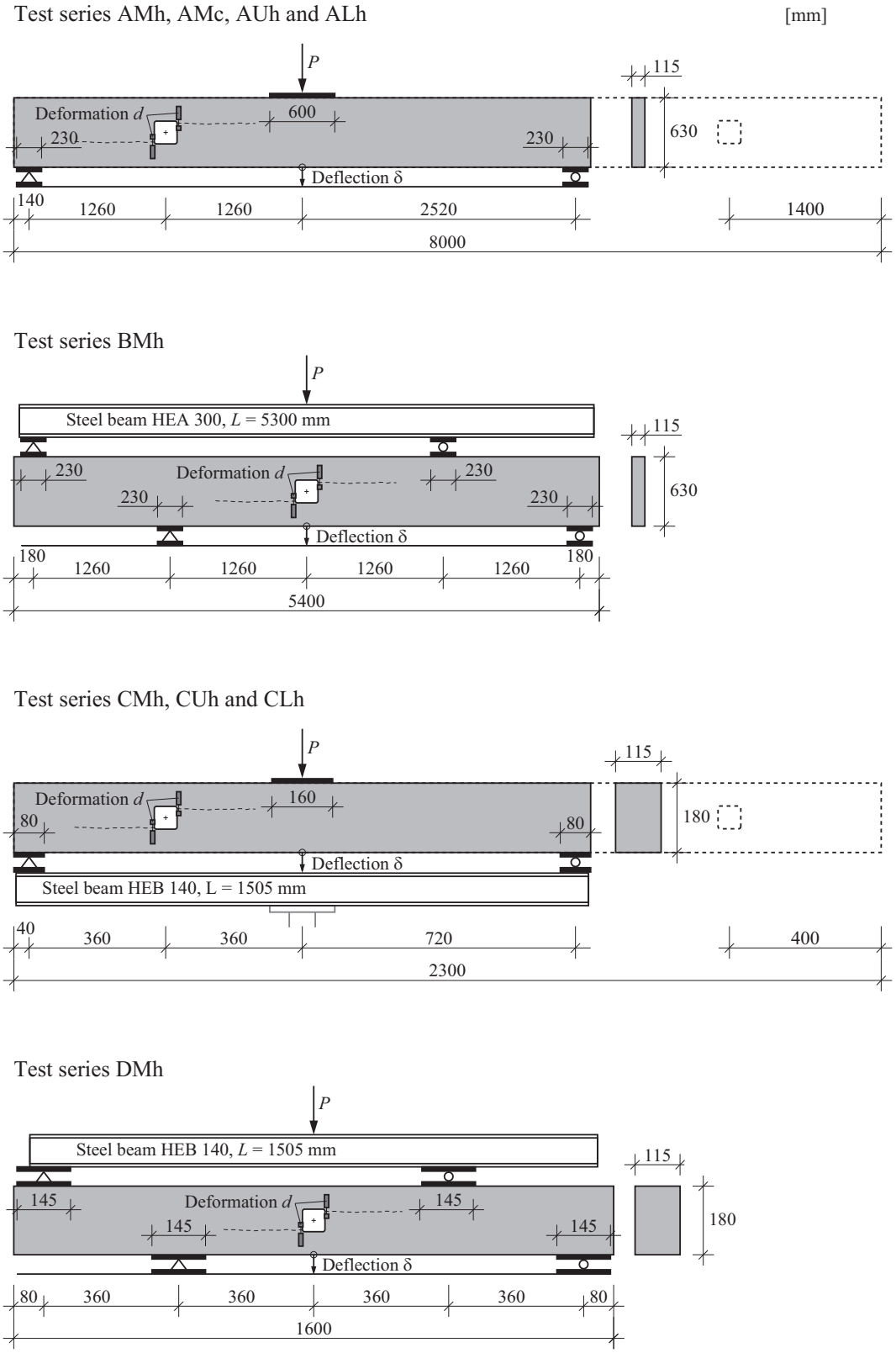

Figure 3: *Test setups with dimensions of glulam beams and steel parts.*

Figure 4: *Photos of the holes and LVDT sensors from test series: AMh, AMc and AUh (top); ALh, BMh and CMh (middle); CUh, CLh and DMh (bottom).*

Figure 5: *Photos of test setups used for test series AMh, AMc, AUh and ALh (top left); BMh (top right); CMh, CUh and CLh (bottom left) and DMh (bottom right).*

3 Materials

All glulam beams were produced and delivered by Töreboda Moelven AB. The beams were made of spruce (Lat. *Picea Abies*), glued with melamine-urea-formaldehyde (MUF) resin and delivered with pre-made holes. The lamella thickness was consistently 45 mm which means that there were 4 lamellae in the small beams (115×180 mm^2) and 14 lamellae in the large beams (115×630 mm^2). All small glulam beams were strength class homogeneous while both strength class homogeneous glulam and strength class combined glulam were represented among the large beams. The strength class combined glulam beams were produced with the three outmost lamellae on each side of lamination strength class LS22 and the remaining eight of lamination strength class LS15. The strength class homogeneous glulam beams were produced with lamination strength class LS22 throughout the entire beam cross section. The lamellae compositions of the cross sections are illustrated in Figure 6 and the material properties for these lamination strength classes are presented in Table 2. These material properties correspond to the requirements of lamella material properties for the different glulam strength classes in SS-EN 1194 [4]. There were no obvious differences in the average width of the growth rings, in the number of knots or any other visually observable property between the two lamination strength classes.

Table 2: *Material properties for lamination strength classes according to [3].*

		LS15	LS22
Characteristic tensile strength	[MPa]	14.5	22
Mean tensile Young's modulus	[MPa]	11 000	13 000
Density, 5^{th} percentile	[kg/m^3]	350	390

The strength class homogeneous glulam beams correspond to glulam strength class GL32h according to SS-EN 1194 [4]. The strength class combined glulam beams correspond to the glulam strength class L40 according to Swedish BKR [2] and this class is usually considered to correspond to GL32c although this class should be composed of LS22 and LS18 according to SS-EN 1194.

The nominal beam cross section sizes 115×180 mm^2 and 115×630 mm^2 are used throughout this report although the real cross section sizes were measured to 114×178 mm^2 and 114×628 mm^2 respectively at moisture content corresponding to the moisture content at the time of testing. Figure 6 shows the arrangement and relative growth ring orientation of the lamellae in the cross sections and also the location of the holes in relation to the location of the glue lines. The placement of the holes and the direction of load was random with respect to the orientation of the growth rings. The holes were not perfectly shaped according to the dimensions in Table 1 although there were no major discrepancies. The corners of the holes in the small beams were however not ideally quarter circular in shape. The hole surfaces were not smoothed in any way.

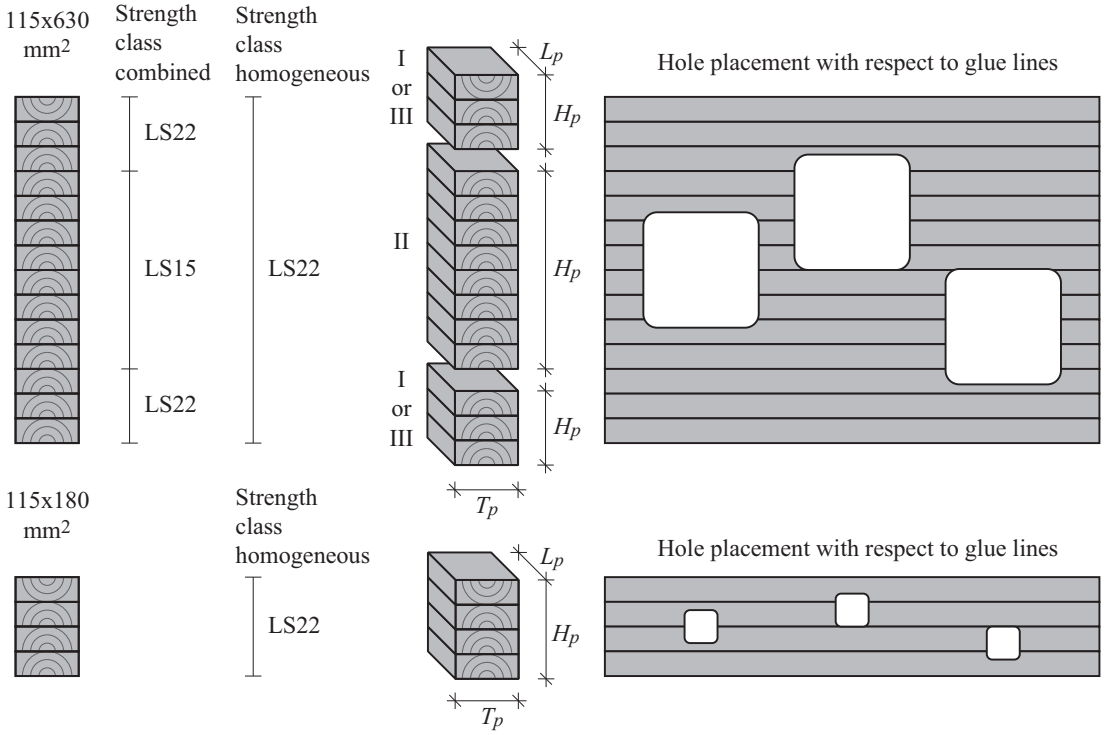

Figure 6: *Illustration of beam cross section composition and hole placement.*

The beams were delivered wrapped in plastic cover and with a moisture content believed to be approximately 12 %. From the time of delivery to the time of testing the beams were kept indoors in a climate of about 20 °C and 35 % RH. The beams were kept in the plastic covers until about ten minutes before testing in order to reduce the risk of any drying and development of any moisture gradient in the material. The moisture content u at time of testing and the density ρ were determined from samples of the tested beams. This was carried out by cutting a piece of length about 100 mm from the beam cross section. The pieces from the large beams where then cut into smaller pieces denoted I, II and III according to Figure 6. The volume V_{test} was determined by measuring the side lengths T_p, H_p and L_p and the mass at time of testing m_{test} was also determined. The pieces were then left to dry in a temperature of 105 °C until the mass was constant and the moisture content was considered to be zero. The moisture content u were for the individual parts determined according to Equation (1) and the mean value according to the same equation with the masses m_{test} and m_{dry} replaced by $\sum m_{test}$ and $\sum m_{dry}$ respectively. The density was determined in the same manner according to Equation (2). The measured data, the moisture content u and the density ρ are presented in Table 3.

$$u = \frac{m_{test} - m_{dry}}{m_{dry}} \qquad [\text{kg/kg}] \text{ or } [\%] \tag{1}$$

$$\rho = \frac{m_{test}}{V_{test}} \qquad [\text{kg/m}^3] \tag{2}$$

Table 3: *Measured data, density ρ and moisture content u at time of testing.*

Test series	no.	piece	T_p [mm]	H_p [mm]	L_p [mm]	m_{test} [g]	m_{dry} [g]	u [%]	ρ [kg/m^3]	
AMh	1,2	I	114	134	100	714.7	638.4	11.95	467.9	
		II	114	359	100	1850.4	1656.7	11.69	452.1	
		III	114	132	99	655.4	593.8	10.37	439.9	
AMh	3,4	I	114	132	100	625.2	565.6	10.54	415.5	
		II	114	359	102	1914.6	1719.3	11.36	458.6	
		III	114	133	101	641.2	579.7	10.61	418.7	
AMc	1,2	I	114	133	99	665.3	595.1	11.80	443.2	
		II	114	360	99	1802.2	1610.5	11.90		443.6*
		III	114	132	99	640.4	571.8	12.00	429.9	
AMc	3,4	I	114	134	98	711.2	633.6	12.25	475.1	
		II	114	360	99	1803.2	1607.1	12.20		443.8*
		III	114	131	100	681.9	610.3	11.73	456.6	
AUh	1,2	I	114	133	101	649.2	586.5	10.69	423.9	
		II	114	359	100	1889.3	1687.7	11.95	461.6	
		III	114	132	101	693.3	620.8	11.68	456.2	
AUh	3,4	I	114	133	102	722.6	649.7	11.22	467.2	
		II	114	360	102	1954.1	1751.5	11.57	466.8	
		III	114	132	101	721.5	648.8	11.21	474.7	
ALh	1,2	I	114	131	92	638.6	574.6	11.14	464.8	
		II	114	359	95	1857.7	1663.1	11.70	477.8	
		III	114	134	99	787.9	704.1	11.90	521.0	
ALh	3,4	I	114	130	94	671.6	601.3	11.69	482.1	
		II	114	359	96	1816.6	1629.5	11.48	462.4	
		III	114	134	99	797.8	709.5	12.45	527.5	
BMh	1	I	114	132	100	768.4	694.5	10.64	510.6	
		II	114	360	100	1876.6	1682.1	11.56	457.3	
		III	114	133	100	735.7	663.1	10.95	485.2	
BMh	2	I	114	133	98	702.2	631.8	11.14	472.6	
		II	114	359	99	1882.2	1675.9	12.31	464.5	
		III	114	132	99	704.6	633.2	11.28	473.0	
BMh	3	I	114	133	99	717.2	641.9	11.73	477.8	
		II	114	359	99	1781.6	1598.9	11.43	439.7	
		III	114	132	99	623.4	564.3	10.47	418.5	
BMh	4	I	114	133	101	765.0	686.1	11.50	499.6	
		II	114	360	99	1883.8	1688.8	11.55	463.7	
		III	114	131	99	749.4	668.4	12.12	506.9	
CMh	1,2		114	178	100	1021.2	908.7	12.38	503.3	
CMh	3,4		114	178	99	944.9	842.3	12.18	470.4	
CUh	1,2		114	178	99	987.6	879.7	12.27	491.6	
CUh	3,4		114	178	101	1065.9	946.9	12.57	520.1	
CLh	1,2		114	178	99	980.4	871.9	12.44	488.0	
CLh	3,4		114	178	100	1029.4	916.8	12.28	507.3	
DMh	1		114	178	99	948.0	845.3	12.15	471.9	
DMh	2		114	178	99	945.6	841.9	12.32	470.7	
DMh	3		114	178	99	960.3	854.6	12.37	478.0	
DMh	4		114	178	100	986.8	879.1	12.25	486.3	
mean								11.73	468.8	443.7*

* = lamination strength class LS15.

4 Results

Three different load levels are used to present and compare the test results:

Crack initiation shear force V_{c0}
Shear force at first crack development visually observable by the naked eye.

Crack shear force V_c
Shear force at the instant of crack development across the entire beam width.

Maximum shear force V_f
Shear force at instant of either a sudden crack propagation or a step-wise stable/unstable crack growth to the end of the beam.

The crack patterns for these load levels are illustrated in Figure 7 and some examples from the tests are given in Figures 8, 9 and 10 where dashed lines have been drawn under the cracks to emphasize their length and location.

The shear forces corresponding to the three definitions above are for all tests presented in Table 4 and Figures 11 and 12. The exact values of the presented shear forces were determined from visual observations during the testing with aid from the recorded beam deflection δ and the deformations d at the cracked corners of the hole. The crack initiation shear force V_{c0} is only given in the cases when there was a visually observable crack in the cross section before there was a crack spreading across the entire beam width at the given corner. The crack shear force V_c is given for both corner B and corner T for all tests. The length of the crack (in the beam length direction) at this level varies between the tests. For some tests, the crack was only one to a few centimeters in the length direction at this load level while other tests showed an instant crack propagation all the way to the end of the beam at this load level. The maximum shear force V_f is not given for test series BMh and DMh since the test setup for these test series is such that this load level is irrelevant. All forces refer to the shear force at hole center due to the externally applied load. The dead weights of the glulam beams are hence not taken into account. The dead weights of the steel beams used in test series BMh and DMh are however included in the presented loads.

The shear force V is plotted vs the beam deflection δ and the deformations d respectively in Figures 13 to 21 for all individual tests. The crack shear forces V_{cB} and V_{cT} for the individual tests are in these figures indicated in by dotted lines. The deformation d_B corresponds to the measurements from the LVDT sensors at corner B and d_T corresponds to measurements at corner T. Some plots lack deformations from one or more of the LVDT sensors at the corners of the holes due to technical problems. The beam deflections δ for test series CMh, CUh and CLh are presented as measured and is hence not compensated for the deflection in the steel beam (approximately 1 mm at $V = 30$ kN) used in the test setup.

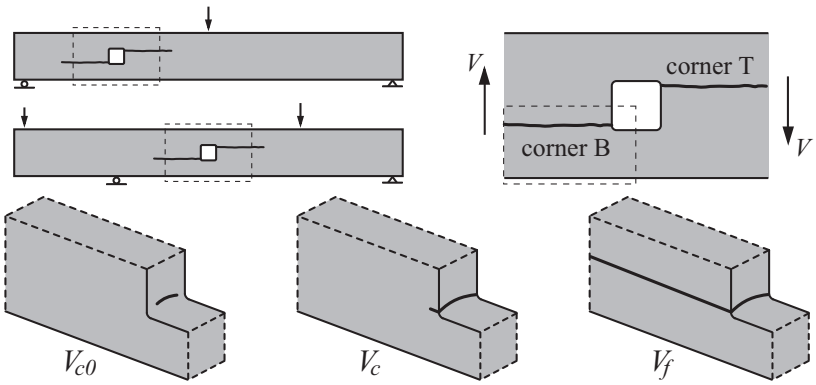

Figure 7: *Illustration of crack patterns for defined load levels.*

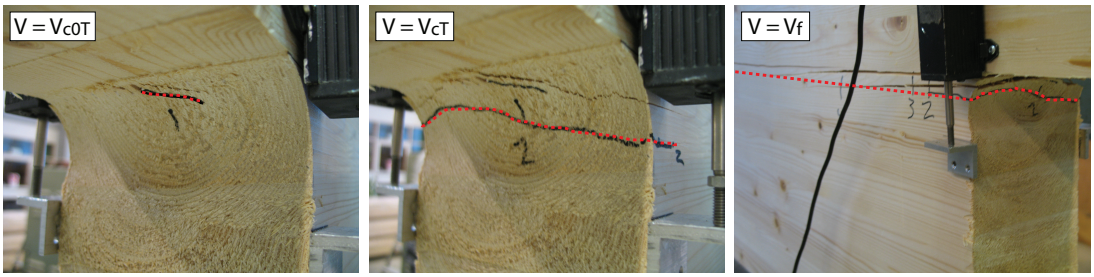

Figure 8: *Photos of crack patterns for corner T of ALh-4.*

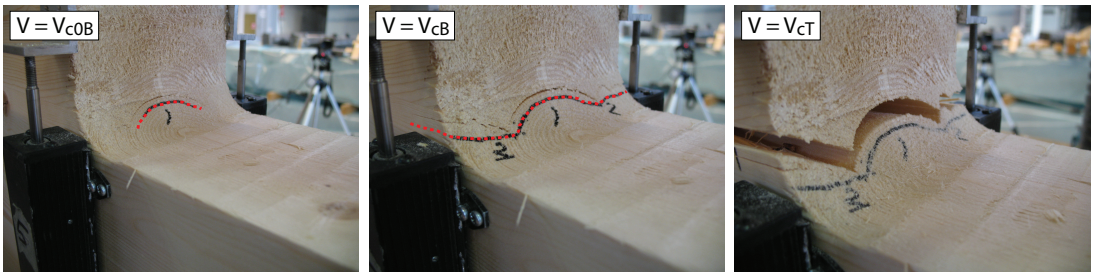

Figure 9: *Photos of crack patterns for corner B of BMh-4.*

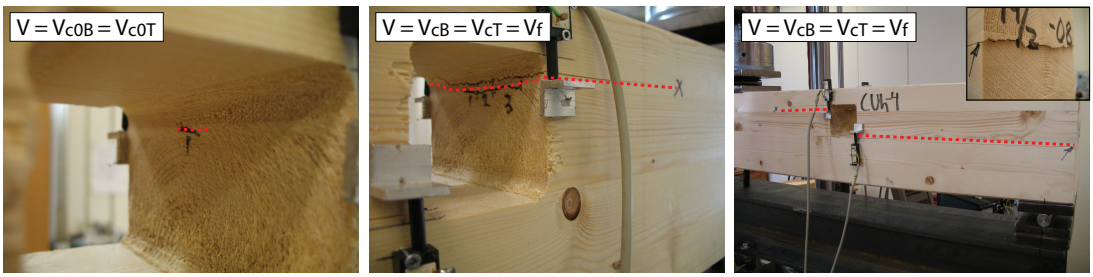

Figure 10: *Photos of crack patterns for CUh-4.*

Table 4: *Shear forces V for all test series.*

		V_{c0} [kN]				V_c [kN]				V_f [kN]	
		V_{c0B}	V_{c0T}	min		V_{cB}	V_{cT}	min			
AMh	1					47.6	45.7	45.7		52.1	
	2	47.5	47.5	47.5		71.4	64.4	64.4		71.4	
	3		42.0	42.0		58.4	58.4	58.4		58.4	
	4					60.5	60.5	60.5		60.5	
	mean (std)			44.8	(3.9)			57.3	(8.1)	60.6	(8.0)
AMc	1	61.0		61.0		64.3	64.3	64.3		64.3	
	2	48.0	44.4	44.4		49.7	51.3	49.7		63.6	
	3	45.0	40.0	40.0		51.2	51.2	51.2		52.8	
	4					49.1	47.7	47.7		54.4	
	mean (std)			48.5	(11.1)			53.2	(7.5)	58.8	(6.0)
AUh	1		28.6	28.6		59.2	57.6	57.6		59.2	
	2					51.6	59.0	51.6		60.5	
	3		55.1	55.1		56.2	56.2	56.2		56.2	
	4	47.5	54.6	47.5		57.4	57.4	57.4		57.4	
	mean (std)			43.7	(13.6)			55.7	(2.8)	58.3	(1.9)
ALh	1	50.2	41.5	41.5		53.9	50.2	50.2		58.9	
	2		43.7	43.7		54.5	52.1	52.1		69.6	
	3		40.0	40.0		64.8	53.2	53.2		64.8	
	4		39.5	39.5		57.0	44.6	44.6		69.8	
	mean (std)			41.2	(1.9)			50.0	(3.8)	65.8	(5.1)
BMh	1		51.9	51.9		61.3	61.3	61.3		-	
	2	59.4	49.0	49.0		65.7	65.7	65.7		-	
	3	61.4	56.0	56.0		62.1	62.1	62.1		-	
	4	48.5		48.5		59.7	68.7	59.7		-	
	mean (std)			51.4	(3.4)			62.2	(2.5)		
CMh	1	20.6	20.6	20.6		27.3	27.3	27.3		27.3	
	2	24.1	23.3	23.3		24.9	24.9	24.9		29.5	
	3	23.1	17.9	17.9		24.4	23.1	23.1		25.3	
	4	24.4	24.4	24.4		27.0	27.0	27.0		27.0	
	mean (std)			21.6	(2.9)			25.6	(2.0)	27.3	(1.7)
CUh	1	24.0	18.8	18.8		25.3	25.3	25.3		25.3	
	2		19.0	19.0		23.2	22.5	22.5		25.3	
	3	20.5	20.5	20.5		23.3	23.3	23.3		23.3	
	4	16.7	16.7	16.7		22.3	22.3	22.3		22.3	
	mean (std)			18.8	(1.6)			23.4	(1.4)	23.6	(2.2)
CLh	1		17.5	17.5		23.1	22.3	22.3		26.9	
	2	19.2	19.2	19.2		23.7	23.7	23.7		29.5	
	3	21.8	23.4	21.8		24.3	24.3	24.3		25.5	
	4					21.8	21.8	21.8		24.5	
	mean (std)			19.5	(2.2)			23.0	(1.2)	26.6	(2.2)
DMh	1	26.0	26.0	26.0		29.1	29.1	29.1		-	
	2					25.3	25.3	25.3		-	
	3	23.3		23.3		25.3	25.3	25.3		-	
	4	25.4	22.6	22.6		26.7	28.1	26.7		-	
	mean (std)			24.0	(1.8)			26.6	(1.8)		

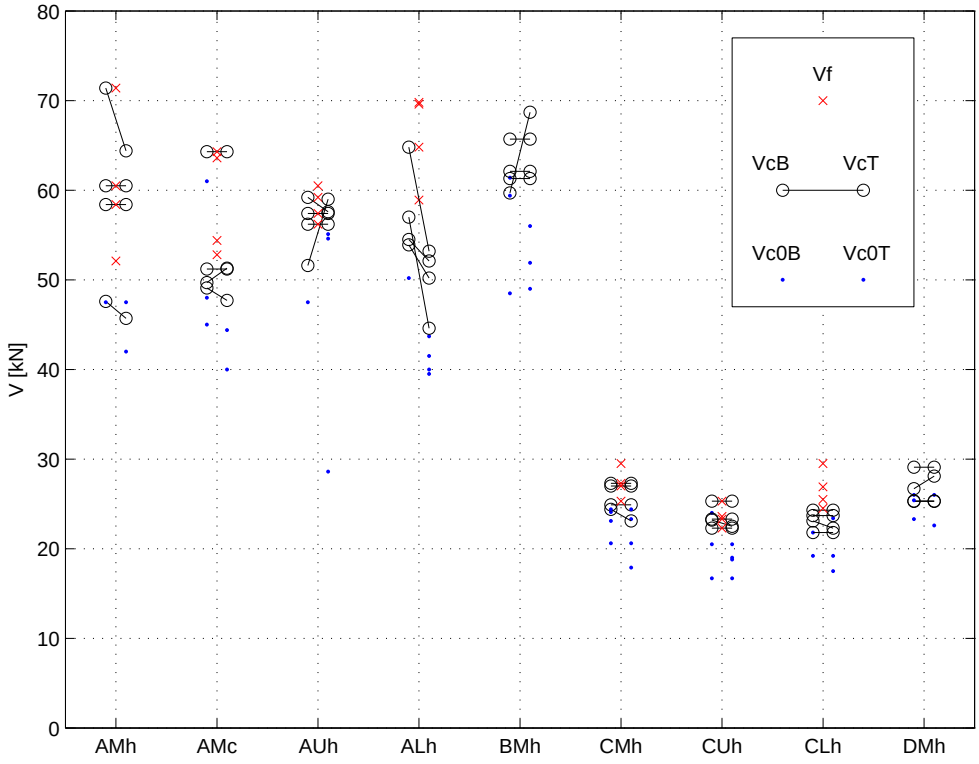

Figure 11: *Shear force V for all test series.*

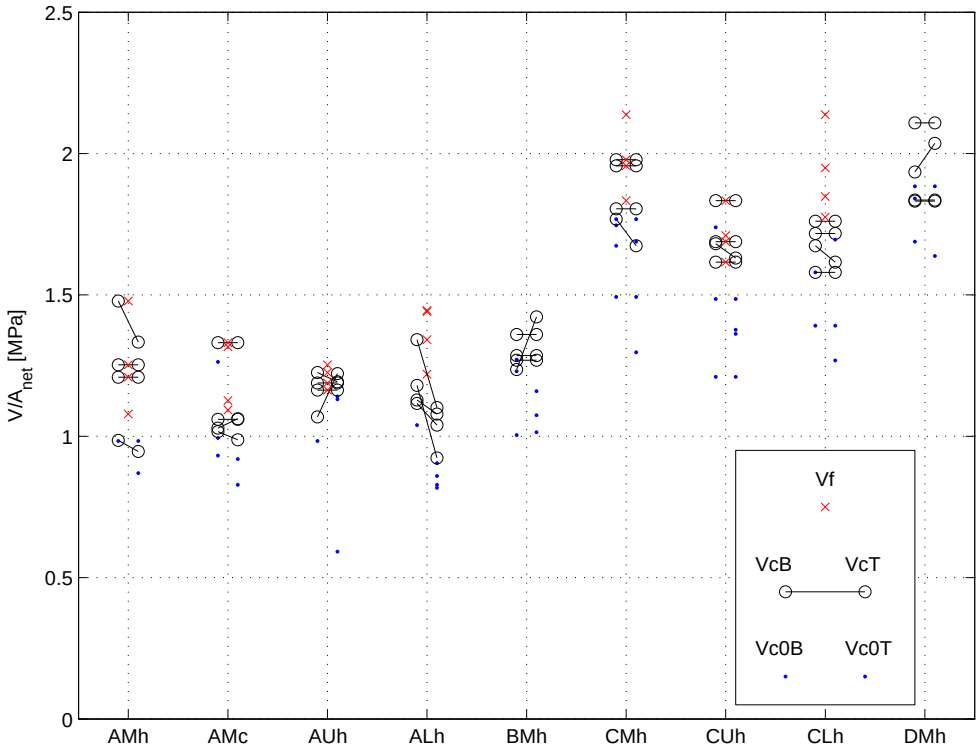

Figure 12: *Mean shear stress $\tau = V/A_{net} = V/((H-b)T)$ for all test series.*

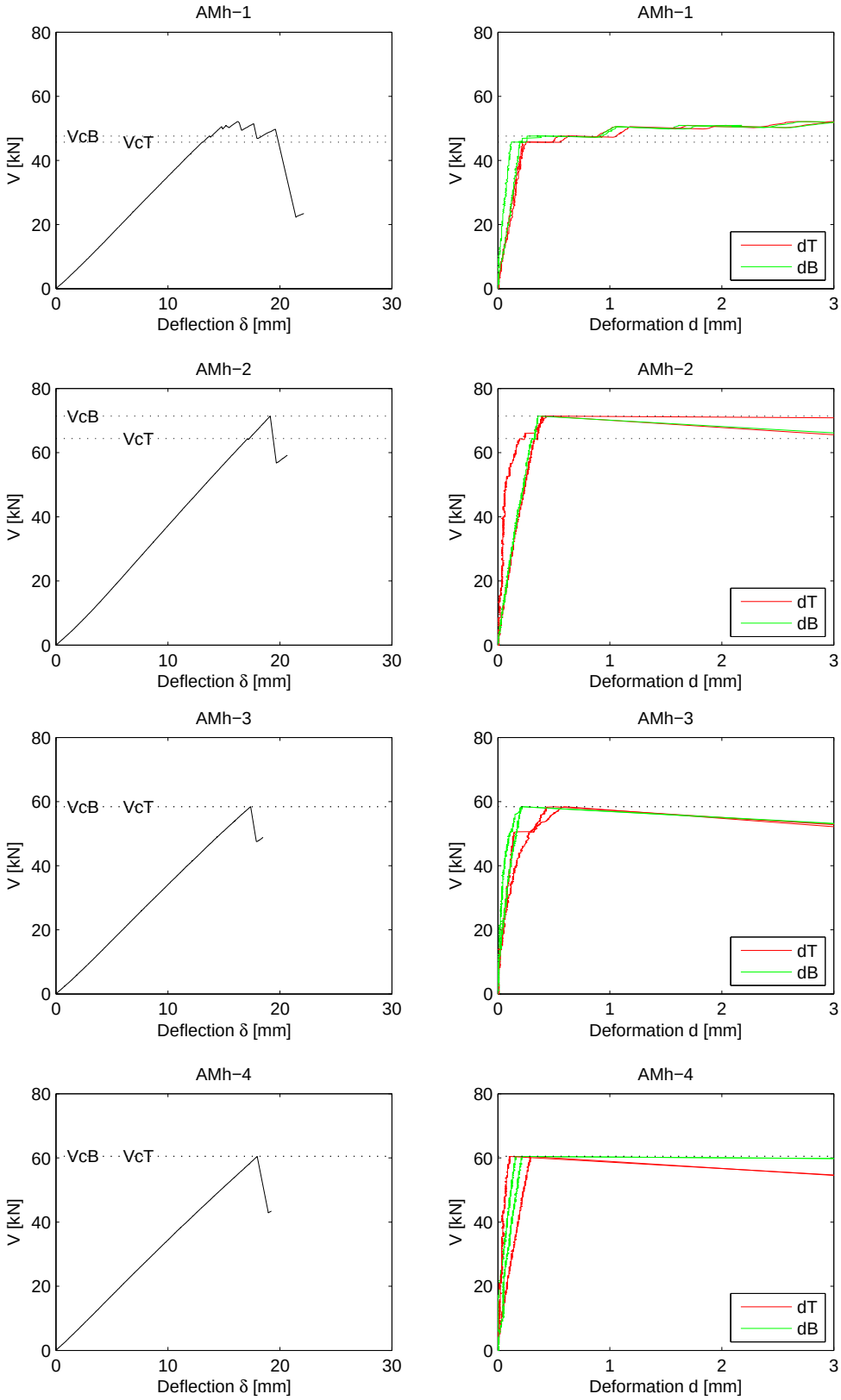

Figure 13: *Deflection δ and deformations d for test series AMh.*

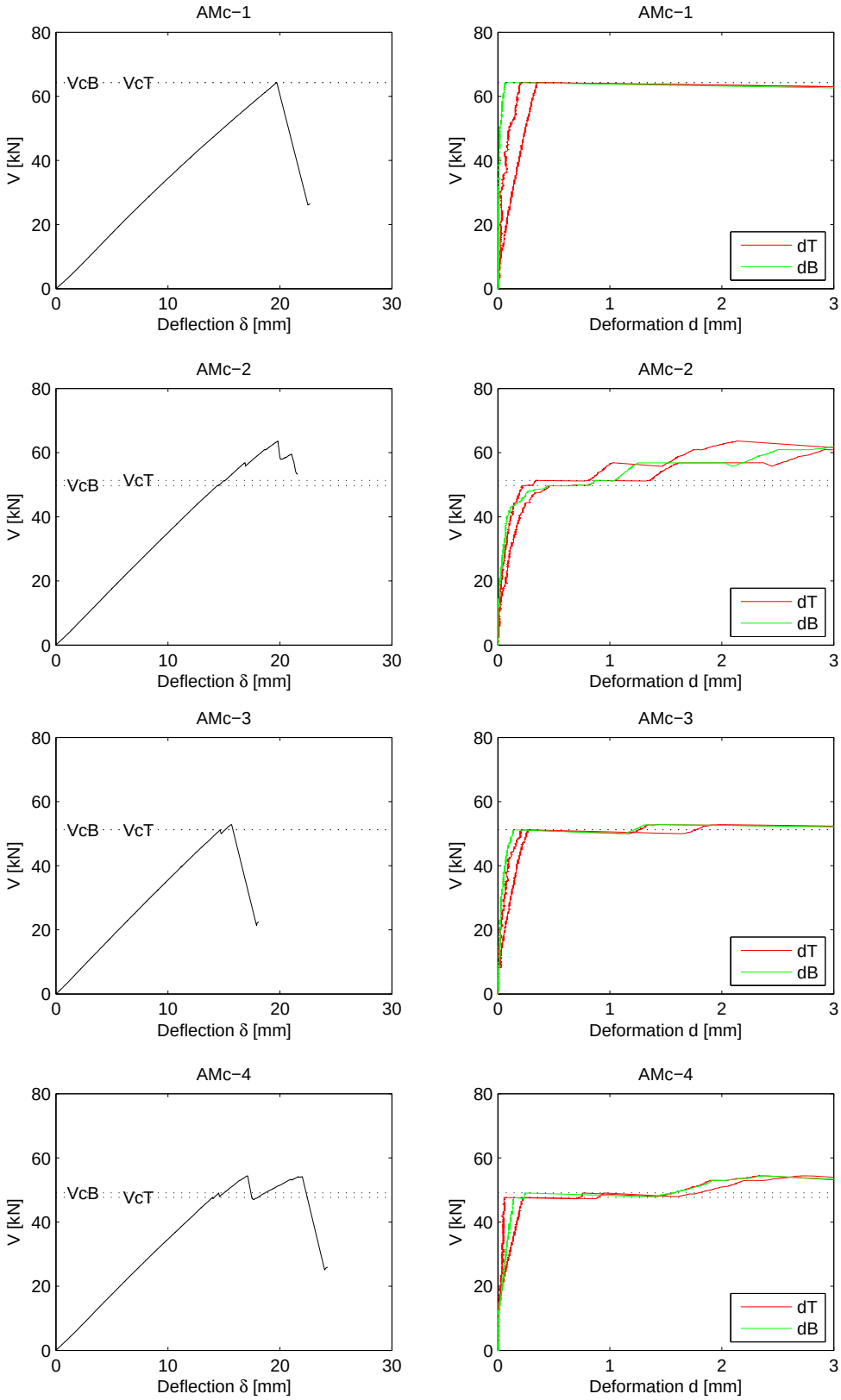

Figure 14: *Deflection δ and deformations d for test series AMc.*

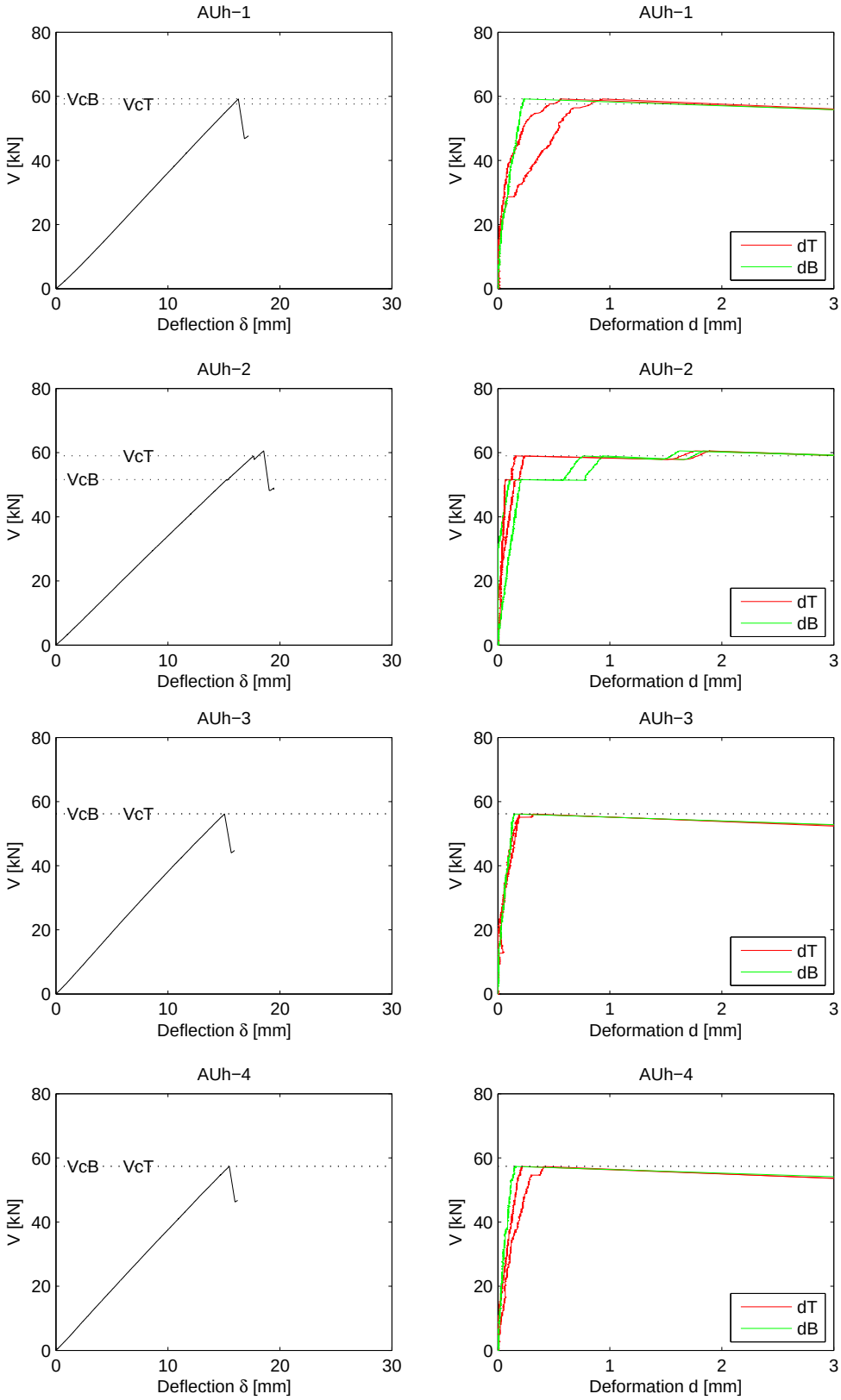

Figure 15: *Deflection δ and deformations d for test series AUh.*

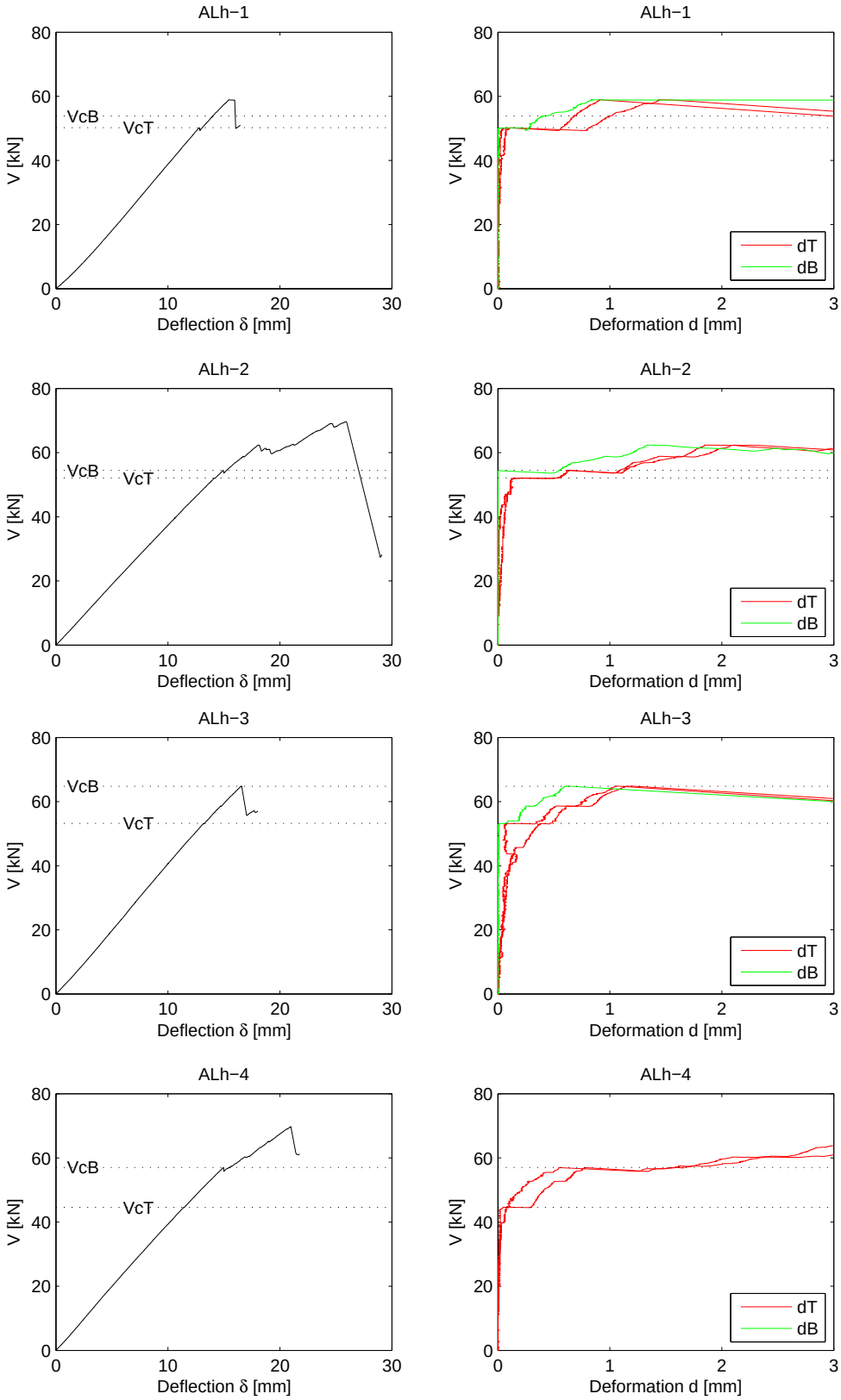

Figure 16: *Deflection δ and deformations d for test series ALh.*

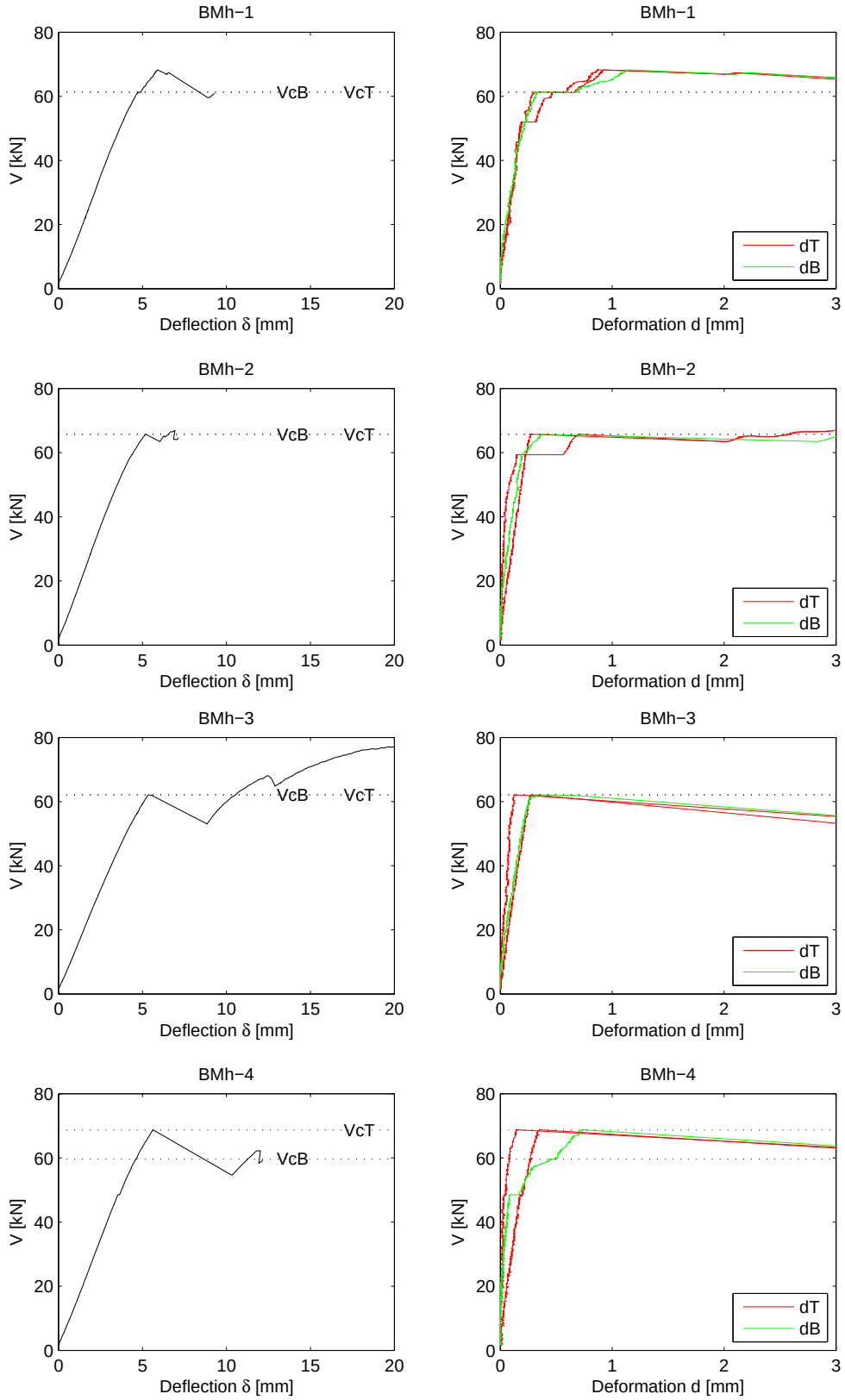

Figure 17: *Deflection δ and deformations d for test series BMh.*

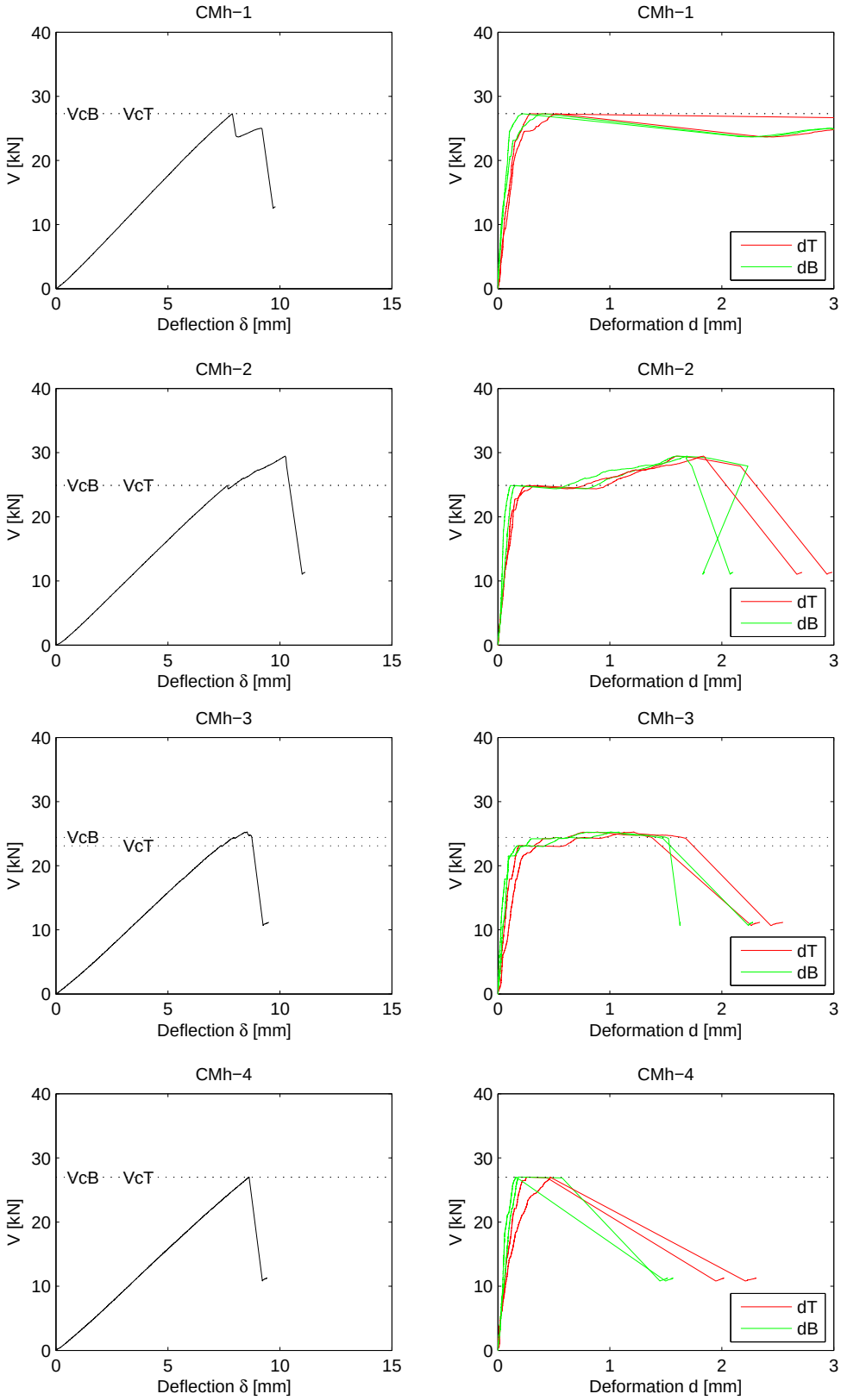

Figure 18: *Deflection δ and deformations d for test series CMh.*

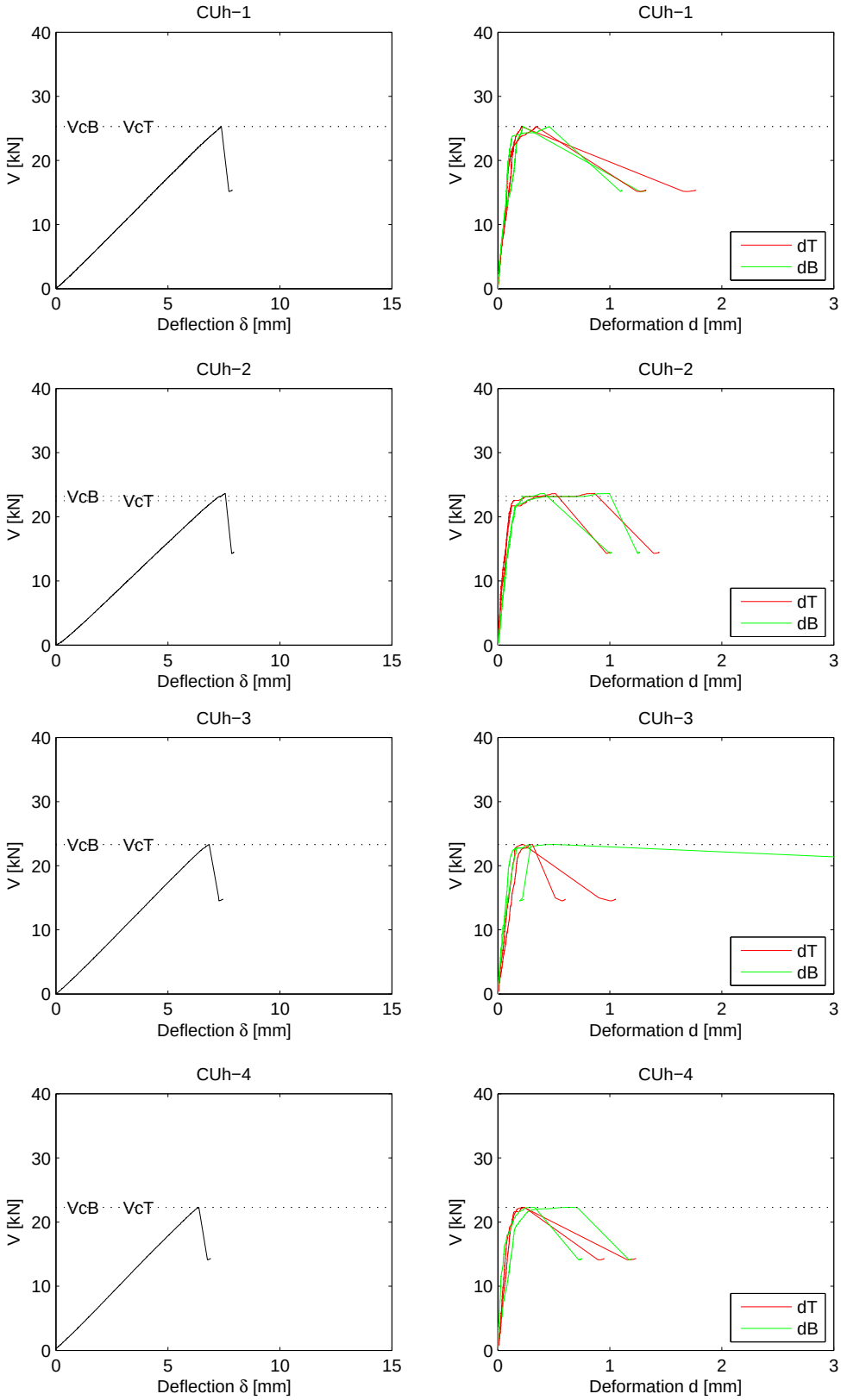

Figure 19: *Deflection δ and deformations d for test series CUh.*

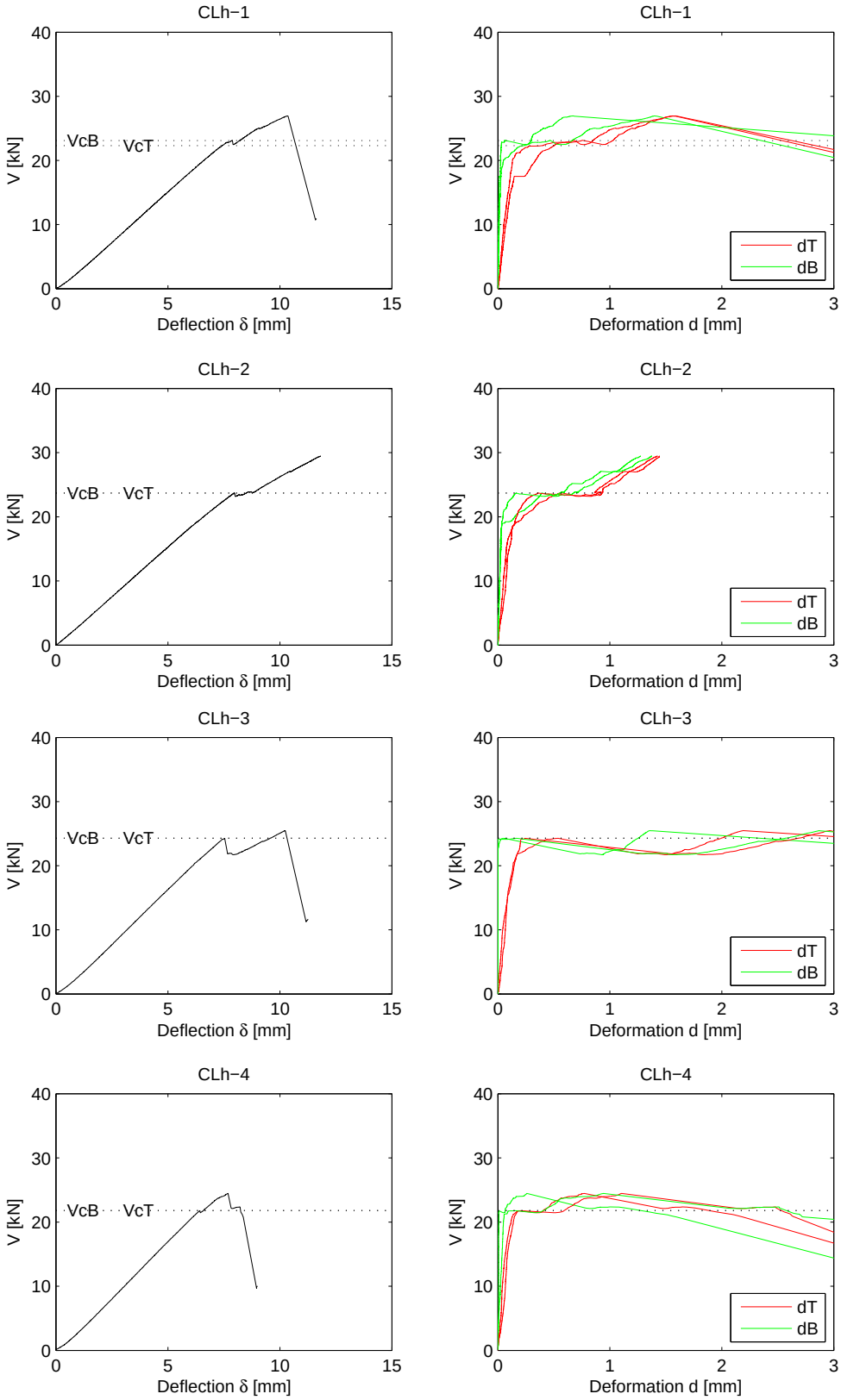

Figure 20: *Deflection δ and deformations d for test series CLh.*

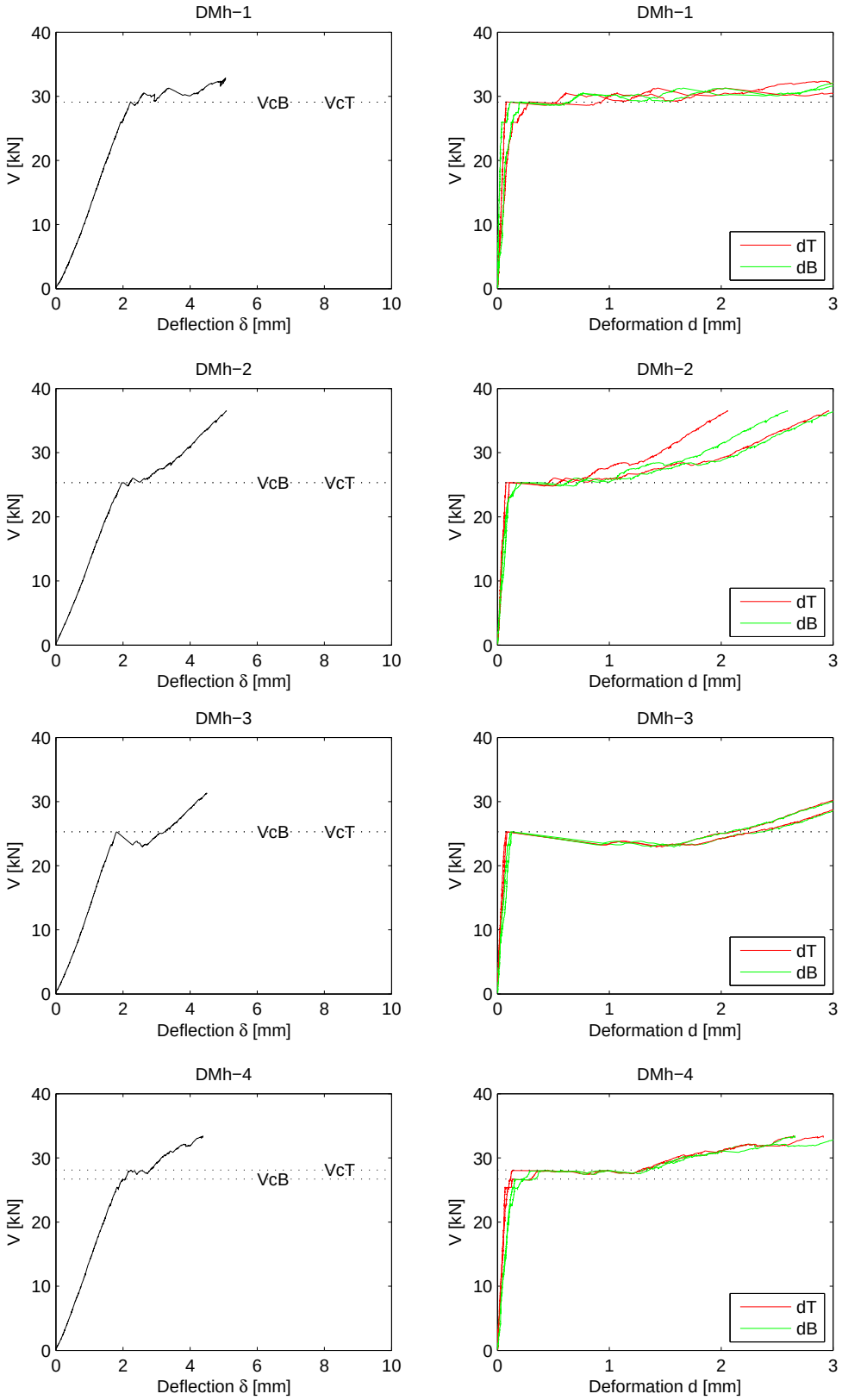

Figure 21: *Deflection δ and deformations d for test series DMh.*

5 Concluding remarks

Some comments on the test results concerning the influence of the four investigated design parameters are listed below.

Beam size

The test results indicate a strong beam size effect on the relative strength as can be seen in Figure 12. Increasing the beam size by a factor 3.5 gave about 30-35 % reduction in nominal shear stress V/A_{net} at the instant of crack development across the entire beam width.

Hole placement with respect to beam height

Slightly lower (approximately 5-15 % considering mean values) crack shear forces V_c were found for the beams with eccentrically placed holes compared to the beams with centrically placed holes. There is furthermore another interesting difference concerning the beams with eccentrically placed holes. Both among the large and the small beams the tests generally showed a more sudden crack propagation all the way to the end of beam for the beams with the hole placed in the upper part of the beam (test series AUh and CUh) compared to the beams with the hole placed in the lower part of the beam (test series ALh and CLh).

Material Strength Class

There was no significant difference in the behavior between the material strength class homogeneous beams of test series AMh and the strength class combined beams of test series AMc. The results of these two test series are however comparatively scattered.

Bending moment to shear force ratio

For beams with centrically placed holes, two different bending moment to shear force ratios where investigated. The beams with holes placed in a position of zero bending moment (test series BMh and DMh) shows on average slightly higher (approximately 5-10 % considering mean values) crack shear forces V_c compared to the beams with holes placed in a position of combined bending moment and shear force (test series AMh and CMh).

The scatter in the strength between nominally equal tests within a test series is not very large, the coefficient of variation of V_c being from 4 % to 14 % with an average of 8 %.

The test results furthermore show that it is more frequent with crack development across the entire beam width (V_c) at the upper corner T before the lower corner B than the other way around. The most frequent scenario is however that cracks develop simultaneously at both corners. The most common place for crack initiation (V_{c0}) is in the middle of the beam width although some tests showed a crack initiation all the way to one side of the beam width.

References

[1] Danielsson H.
The Strength of Glulam Beams with Holes – A Survey of Tests and Calculation Methods
Report TVSM-3068, Division of Structural Mechanics, LTH, Lund University, 2007.

[2] Boverket
(The National Board of Housing, Building and Planning)
Regelsamling för konstruktion – Boverkets konstruktionsregler BKR.
(Design Regulations)
Elanders Gotab, Vällingby, 2003.

[3] SP Sveriges Provnings- och Forskningsinstitut
(SP Swedish National Testing and Research Institute)
Lamination strength classes for glued laminated timber according to EN 1194.
PM, 2002-06-14.

[4] SS-EN 1194:1999
Träkonstruktioner – Limträ – Hållfasthetsklasser och bestämning av karakteristiska värden.
(Glued laminated timber – Strength classes and determination of characteristic values.)
SIS Förlag, Stockholm, 2000.